Characterizing Single Ventricle Patient-Specific Anatomy Using Segmentation of MRI and 3D Reconstruction to Aid Surgical Planning

By

Jayaprakash, Gopinath

Georgia Institute of Technology Cardiovascular Fluid Mechanics Laboratory
Fontan Division

Undergraduate Research Opportunities Program (UROP) Thesis

Summer, 2008

Mentor: Sundareswaran, Kartik
Program Director: Yoganathan, Ajit P.
Faculty Mentor: Williams, Douglas B.

Abstract **–** Single ventricle congenital heart defects occur 2 per every 1000 live births in the USA. In these cases, cyanosis occurs due to the mixing of venous deoxygenated blood and oxygenated blood from the lungs. These defects are surgically treated by the total cavo-pulmonary connection (TCPC), where the superior and inferior vena cavae are connected to the pulmonary arteries routing the systemic venous return directly to the lungs. However, this Fontan repair results in high energy losses and therefore the optimization of this connection prior to the surgery could significantly improve post-operative performance. In this paper, the in-house segmentation and 3D reconstruction scheme is used in the following studies. First, 3D geometrical analysis of the TCPCs is used to determine the advantages and disadvantages of two commonly performed TCPC palliations – intra-atrial and extra-cardiac configurations. Then, a surgical planning outline is proposed with segmentation of pre and post surgical Magnetic Resonance Imaging (MRI) data followed by the 3D reconstruction with emphasis on extracting surrounding vessels and structures. A pediatric surgeon performs a 'virtual surgery' on the reconstruction of the patient's pre-Fontan anatomy prior to the actual surgery. A segmentation of the heart, aorta and surrounding vessels superimposed with the Glenn, when used with the SURGEM® tool, simulates the actual Fontan operation. This outline allows the surgeon to envision numerous scenarios of possible surgical options, and accordingly to predict the post operative procedures. The segmentation tool is improved upon to increase the accuracy and efficiency of the process and enhance the quality of the anatomical reconstructions.

Index Terms – Fontan, Surgical Planning, MRI, TCPC, Glenn

A) Introduction

With about two thousand incidences of children born in the United States with single ventricle congenital heart defects per year, Fontan repairs are palliative improving the lifespan of such patients tremendously over the years. However, the procedure is not remedial. In patients with such an anatomy, oxygenated and deoxygenated blood mix in the single ventricle. This is called venous blood mixing. The total right ventricular bypass, first introduced by Fontan and Baudet in 1971[2], is a surgical procedure aimed at separating the systemic and pulmonary circulations thus eliminating venous blood mixing. The current Fontan procedure is the total cavopulmonary connection (TCPC) that is performed to correct major Congenital Heart Defects (CHD), such as Hypoplastic Left Heart Syndrome (HLHS) and Tricuspid Atresia.

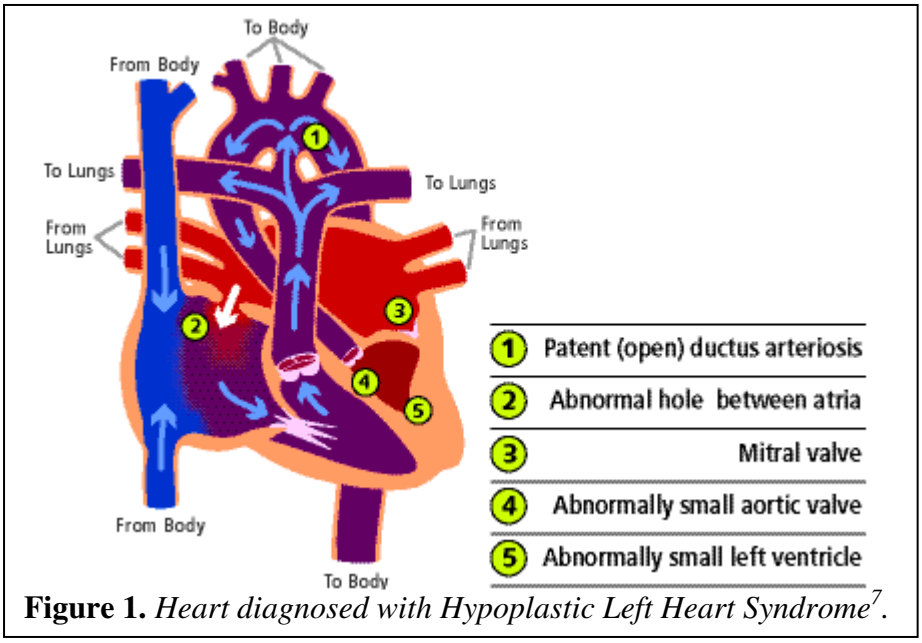

Figure 1. *Heart diagnosed with Hypoplastic Left Heart Syndrome*[7].

In HLHS, for unknown reasons, the left side of the heart does not develop properly during gestation. The parts of the heart that are usually affected are the mitral valve (1), the left ventricle (2), the aortic valve (3), and the aorta (4). In the normal heart, red blood returning from the lungs, flows from the heart's left upper chamber called the left atrium through the mitral

valve to the left ventricle where it is pumped through the aortic valve and out to the body (sees Figure 1). In babies with HLHS, the left side of the heart is underdeveloped and cannot pump enough blood to meet the body's needs.

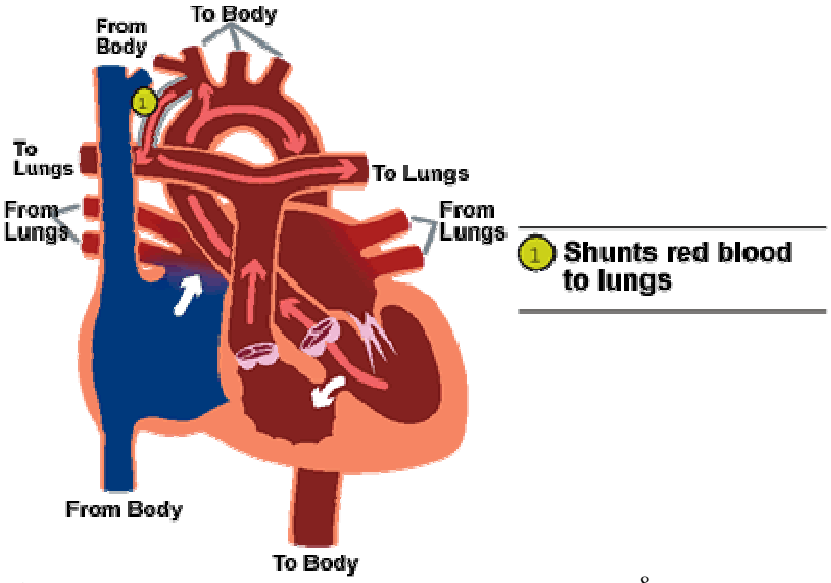

Figure 2. *Heart diagnosed with Tricuspid Atresia*[8].

In the normal heart, the tricuspid valve is located on the heart's right side between the atrium (the upper chamber) and the ventricle (the lower chamber). In babies born with Tricuspid Atresia (see Figure 2), the tricuspid valve is absent (1) and the right ventricle is small (2). In about 25% of babies, the position of the great arteries is also reversed. In some babies, there is also a severe narrowing at the pulmonary valve (3), or complete absence of the pulmonary valve. In all babies with tricuspid atresia, there is no direct pathway for blue blood returning from the body to get to the lungs to pick up oxygen.

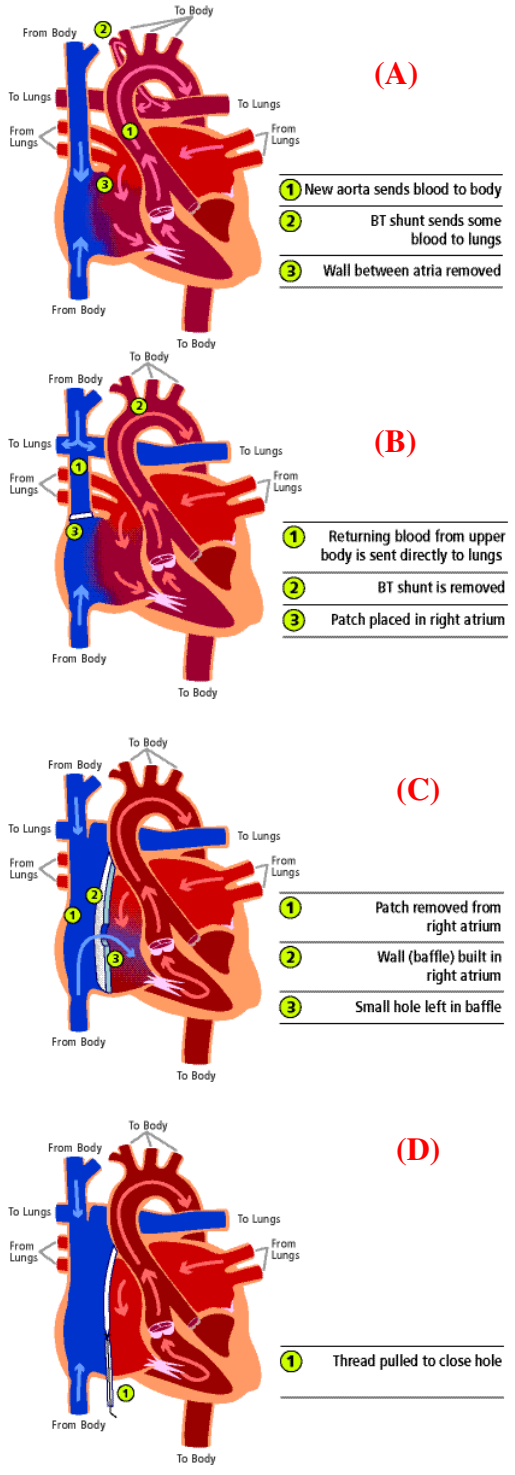

Figure 3. *Norwood (A), Glenn/Hemi-fontan (B), Fontan (C), and Fontan Fenestration closure procedures to correct HLHS*[7].

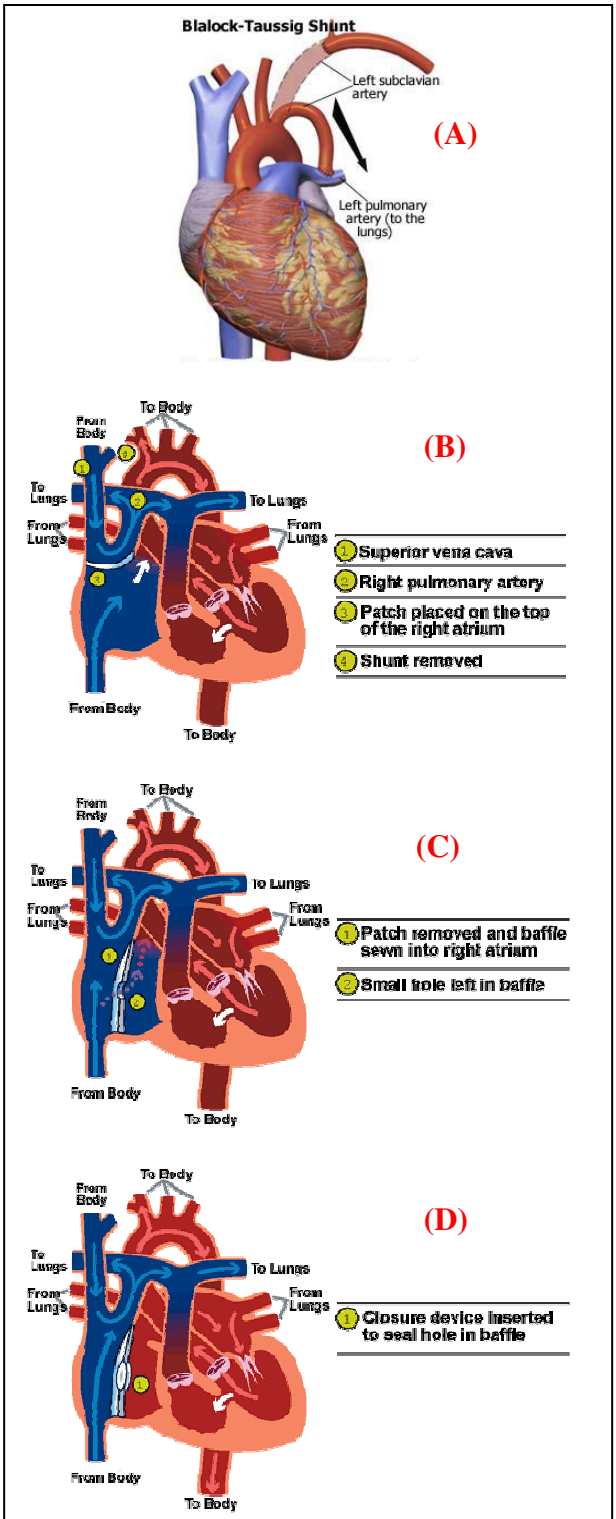

Figure 4. *BT shunt (A)*[2]*, Glenn/Hemi-fontan (B), Fontan (C), and Fontan Fenestration closure procedures to correct Tricuspid Atresia*[8].

The Fontan operation involves a series of three palliative procedures aimed separating the systemic and pulmonary circulations and reducing the long term effects of chronic hypoxia and ventricular volume overload. The first stage is the Norwood procedure, first introduced in 1980, (Figure 3A) and performed in the neonatal period with a systemic to pulmonary artery shunt followed by an aortic reconstruction when needed. In the second stage the SVC is anastomosed to the pulmonary arteries in a bidirectional cavopulmonary connection (BCPC) configuration (Figure 3B). The total cavopulmonary connection (TCPC) is completed in the final stage of the surgery with the anastomosis (joining together of two hollow organs (viscous), usually to restore continuity after resection, or to bypass an unresectable disease process) of the inferior vena cava (IVC) to the BCPC (Figures 3C and 3D).

The Blalock-Taussig Shunt (BT) procedure is performed, instead of the Norwood operation, on patients with Tricuspid Atresia; the BT involves sewing a Gortex tube between the subclavian (right arm) artery and the right pulmonary artery (Figure 4A). Through this tube, a fixed amount of blood reaches the lungs with each heartbeat. Ultimately, these three procedures result in the connection of the inferior (IVC) and superior (SVC) vena cavae directly onto the pulmonary arteries (PAs) thus bypassing the right side of the heart.

In the third stage of the operation, where the separation of the pulmonary and systemic circulation is achieved, the venous blood (deoxygenated blood) from the rest of the body goes to the lungs via the pulmonary arteries. After being oxygenated, the blood goes into the heart via the pulmonary veins and gets pumped out to the rest of the body via the single right ventricle. In this procedure, the two commonly used techniques are the intra-atrial and extra-cardiac conduit connections.

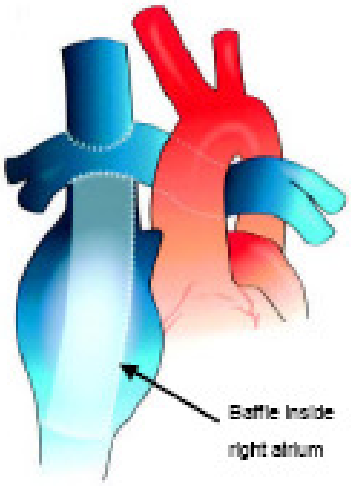

Figure 5. *Diagram of an intra-atrial TCPC*[12].

In intra-atrial connections, the right atrium is connected to the RPA using the right atrial appendage as shown in Figure 5. Then, a baffle is placed within the right atrium to allow venous blood to flow along the right side of the baffle toward the pulmonary arteries bypassing the heart.

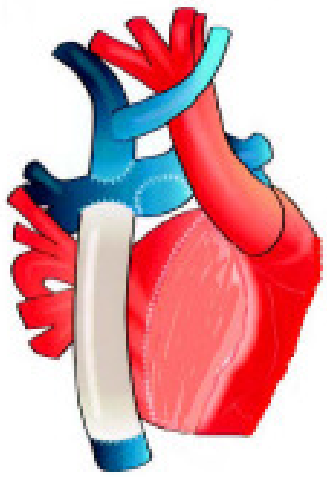

Figure 6. *Diagram of an extra-cardiac TCPC*[12].

In extra-cardiac connections, the venous blood from the rest of the body via the IVC is routed sround the heart. The IVC is disconnected from the right atrium and anastomosed to the RPA with a synthetic graft as shown in Figure 6.

The choice of either intra-atrial or extra-cardiac procedures for the 3rd stage operation depends on the surgeon's preference and both have balanced pros and cons. The intra-atrial option provides limited pulsatility to the IVC flow through the pumping action of the right atrium, but the patient faces the risks of sinus-node damage and resulting arrhythmias. Extra-cardiac TCPC have smoother geometries, less atrial damage and the patient spends less time on the heart/lung machine. However, there is no growth potential, and this may lead to conduit stenosis and throboembolism[13, 14, 15]. **To better understand the advantages and disadvantages of extra-cardiac or intra-atrial lateral tunnel technique, segmentation and 3D reconstruction of patients' MRI data is performed to produce TCPC geometries.**

Figure 7 shows the schematic of a typical TCPC geometry after the third stage has been completed. This schematic is very general as there are many variations. For the 3rd and last stage alone, two major surgical procedures can be identified to connect the IVC and the RPA joint with the bidirectional cavopulmonary shunt: extra-cardiac conduits going around the heart and intra-atrial tunnels going through the right atrium. Within these two types are several variations that include offsetting of the caval connections on the right pulmonary artery, flaring of the connection sites and use of different graft materials. Standardization of geometric designs of the TCPC and materials used has not occurred and the choice of TCPC procedure solely depends on the surgeon's preference and personal discretion. Providing a rationale to select one option over the other would be desirable, particularly for the range of anatomical and surgical variations that are encountered in clinical practice.

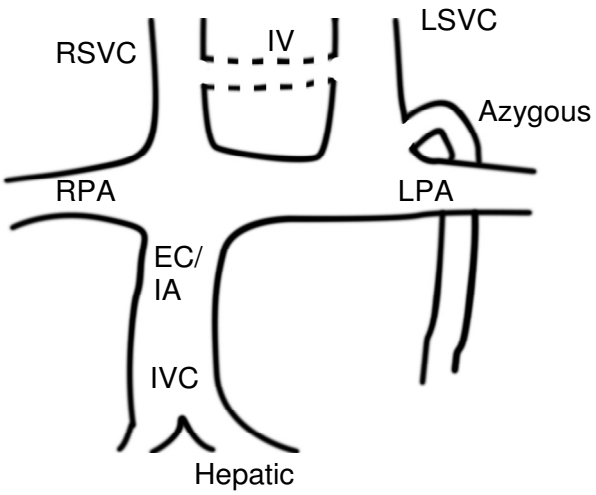

Figure 7. *The 2D geometry of a typical TCPC.*

Different techniques have been employed to understand the TCPC hemodynamics and geometrical features. These include *in vivo* modalities like echocardiography and MRI in the medical industry. To name a few, Shiota et al. reported the use of high-resolution echocardiography for studies the intra cardiac structures of CHD patients[16]. In 1995 Fogel et al. performed a detailed study on SV patients after the Fontan operation using MRI tagging to understand the effect of this surgery on the myocardial functioning of the patients[17]. They found significant differences in the myocardial strain of the patients between the three Fontan stages. In another study, Fogel et al. were able to characterize the contribution of each vena cava to each one of the pulmonary arteries in 10 Fontan patients with intra-atrial tunnels[18]. In agreement with previous findings, they found that at an average age of 2 year-old most of the caval flow from the SVC, 60±6% went to the RPA, and 67±12% of the IVC blood went to the LPA[19]. Be'eri et al. used phase-contrast MRI to demonstrate the advantages of TCPC over an AP connection[20]. Sharma et al. analyzed the flow characteristics seen in intra atrial TCPC using MRI[21]. Flow

structures with twelve different patients, 7 of which were intra-atrial and 5 of which were extra-cardiac, were reported using interpolation methods that were able to produce *in vivo* velocity data[22]. This was used to compute energy dissipation and calculate power loss in TCPC geometries[23]. Over the past decades, experimental and numerical models have incorporated increasing levels of geometrical complexity in an effort to more accurately model the in vivo conditions. However, these have failed to establish the general conclusions due to the complexity and number of the geometrical features that need to be taken into account. There is now a need for systematic analysis methodology that will allow for the identification of crucial geometrical parameters (such as vessel diameter) and their correlation with the TCPC performances.

Unfortunately, these repairs are mollifying and not healing. Survivors often require a lifetime of intensive medical attention. Clinicians report that over 50% of their time must be devoted to the 20% of their patients having this complex cardiovascular physiology. Due to the absence of the right ventricular pump, Fontan patients have hypertension in the systemic return so as to provide the pressure head necessary to drive the flow through the pulmonary circuit and back to the left side of the heart. This pressure build up leading to power losses in the TCPC may be a possible explanation for the complications typically observed in these patients, including limited exercise capacity, congestive heart failure, liver dysfunction, protein losing enteropathy, systemic venous hypertension, hepatic and pulmonary congestion, and valvular and myocardial dysfunction.

Surgeons are looking for problems associated with the Fontan procedures that they can solve, and one of these is the design of the surgically created connection. Significant work has been done in understanding the fluid dynamics of the TCPC, underscoring the tight relationship between design and associated pressure drops and energy dissipation. However, no work to date

has been done towards a systematic surgical planning of the TCPC. There is a need to optimize its design for every single patient, in an effort to reduce pressure losses and improve their long-term outcome. **To facilitate surgical pre-planning, the research consists of segmentation and 3D reconstruction of the complex cardiovascular anatomy with emphasis on extracting surrounding vessels and structures in the patient.**

Specific Aim 1:

- **Segment interpolated patients' MRI data to create a database of 3D TCPC geometries**
    - **Compare intra-atrial and extra-cardiac geometries**
- **Improve the efficiency of the segmentation process with constant upgrading made to the tool**

Literature reviews show that, so far there exists no quantification of the geometric characteristics of the complex Fontan geometries. Geometrical analysis, developed with the centerline approximations of the TCPCs, in our study to determine the differences between two commonly performed TCPC palliations – intra-atrial and extra-cardiac. Significant differences between intra-atrial and extra-cardiac TCPCs can be quantified by applying a shape analysis approach. A modification of the commonly used skeletonization technique, iterative adjustment of the centerline method, is used in this study[24]. The basic principle of this method is to "slice" the geometry of interest into a series of frames and then define the geometric centerline as the line that connects the center of mass of each frame. 3D reconstructions that are represented as triangulated 3D surface geometries will be reduced to their centerline approximations. In addition, this method also correlates some of the important geometrical parameters of TCPC like

the vessel dimensions with the TCPC hemodynamics, especially the power loss. The technique will be applied to a stack of *in vivo* 3D PC MRI images obtained from both intra-atrial and extra-cardiac Fontan patients.

Specific Aim 2:

- **Segment all surrounding structures of interest including the Glenn or TCPC to obtain pre-Fontan and post-Fontan complete 3D reconstructions respectively**
- **Develop the segmentation process in order to segment all structures of interest in a timely fashion**
- **Increase the quality of the anatomical reconstructions which is critical for the accuracy of surgical planning of the TCPC**

The TCPC efficiency has been shown to highly depend on its geometry, which is the result of the surgeons' habits and conventions when doing the Fontan surgery. As such, the clinical implementation of a surgical planning tool that would enable surgeons to visualize patients' anatomies pre-operatively and allow them to test different surgical options ahead of time may help in their design and may have significant benefits on long-term patients' outcomes. But to date, we lack a dynamic and efficient modeling tool that will allow quick reconstructing of the patient's anatomy from medical images (such as Magnetic Resonance (MR)) images, exploration and editing the reconstructed anatomy to perform virtual surgeries to determine further the precision of the pre-surgical planning with respect to the similarity in the results.

The goal of this task to begin developing computer models by efficiently performing segmentation and 3D reconstruction of the vessels that account for the Fontan connection

(pulmonary arteries and venae cavae) and the surrounding anatomical structures (heart, aorta and pulmonary veins). This is critical towards the ultimate goal of surgical planning, which is one of the aims of the grant (National Heart and Lung Blood Institute Grant *HL67622*). Indeed, 3D visualization gives surgeons a clear advantage over viewing just MRI data or operating on the patient with the posterior view only. However, for the surgeon to envision different realistic surgical scenarios, he not only needs to accurately visualize the vessels of interest but also the surrounding constraining structures. To this end, with the assistance of Dr. Rossignac, in Georgia Tech's College of Computing, and his team, a tool (SURGEM®[6]) has been developed to manipulate the 3D model of the reconstructed patient's cardiovascular system and try out different surgical configurations[3]. This would enable the concept of 'virtual surgery' to be possible before the actual operation is performed on the patient.

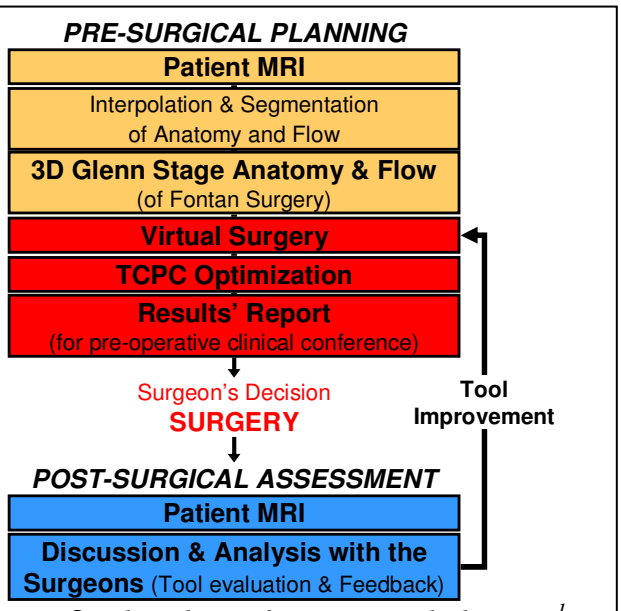

Figure 8. *Flowchart of pre-surgical planning*[1].

Summary:

This paper describes the (Specific Aim 1) the comparison study being performed between intra-atrial and extra-cardiac TCPCs based on the 3D geometrical analysis. In this study, I

segmented patients' MRI to create a database of intra-atrial and extra-cardiac TCPCs using an in-house segmentation tool and then reconstructing 3D geometries. The paper also includes (Specific Aim 1) surgical planning methodology in detail, taking the example of a patient with known pre and post-Fontan cardiac anatomy. I reconstructed pre- and post-cardiac anatomies from MRI with emphasis on extracting surrounding vessels and structures to aid surgical planning. A pediatric cardiac surgeon was blinded to the actual post-operative anatomy and asked to virtually connect the IVC to the pulmonary arteries. I also modified and improved upon the in-house segmentation program to speed up the segmentation process.

Overall, the segmentation and 3D reconstruction scheme is applied in both studies in this research. 3D TCPC geometrical analysis of intra-atrial and extra-cardiac TCPCs will enable better understanding of the optimization of the corrective Fontan procedure by studying power losses in the baffle regions between the two techniques. Pre-Fontan (Glenn) and post-Fontan (TCPC) segmented together with the surrounding heart and vessels can be manipulated to try out different surgical scenarios thus enabling better visualization and paving the way for the future of surgical planning.

B) *Specific Aim 1:* Comparison of 3D Geometries Between Intra-Atrial and Extra-Cardiac TCPCs

Two variations of the TCPC commonly performed by the surgical community are the: intra-atrial (IA) connection where the IVC is anastomosed to the pulmonary arteries using a part of the right atrium; and the extra-cardiac (EC) connection where the IVC is routed around the heart with the help of an artificial conduit. There is no consensus currently in the surgical community as to which one of the two is superior. Each has its own advantages with the intra-

atrial (IA) connection allowing for growth as the patient grows older, while the extra-cardiac conduit has a more streamlined flow structure as a smooth conduit is used.

An approach of central line estimation of the 3D geometrical models has been used to achieve this goal. I provided the 3D segmentations of a database of TCPCs for this study where geometry slicing and centroid calculation was done to build the centerline of the geometries[26]. This is more precise in determining the trend in the properties of the TCPC geometries as compared to just viewing them. The 3D TCPC geometries were classified according to their diagnosis and classification depending on the data received from the hospitals. The segmentations were checked and approved by visiting pediatric cardiac surgeons for details and integrity based on the MRI data and their expertise.

The reconstruction step (Figure 9) is a major one as it conditioned all the others and will be the focus of this project.

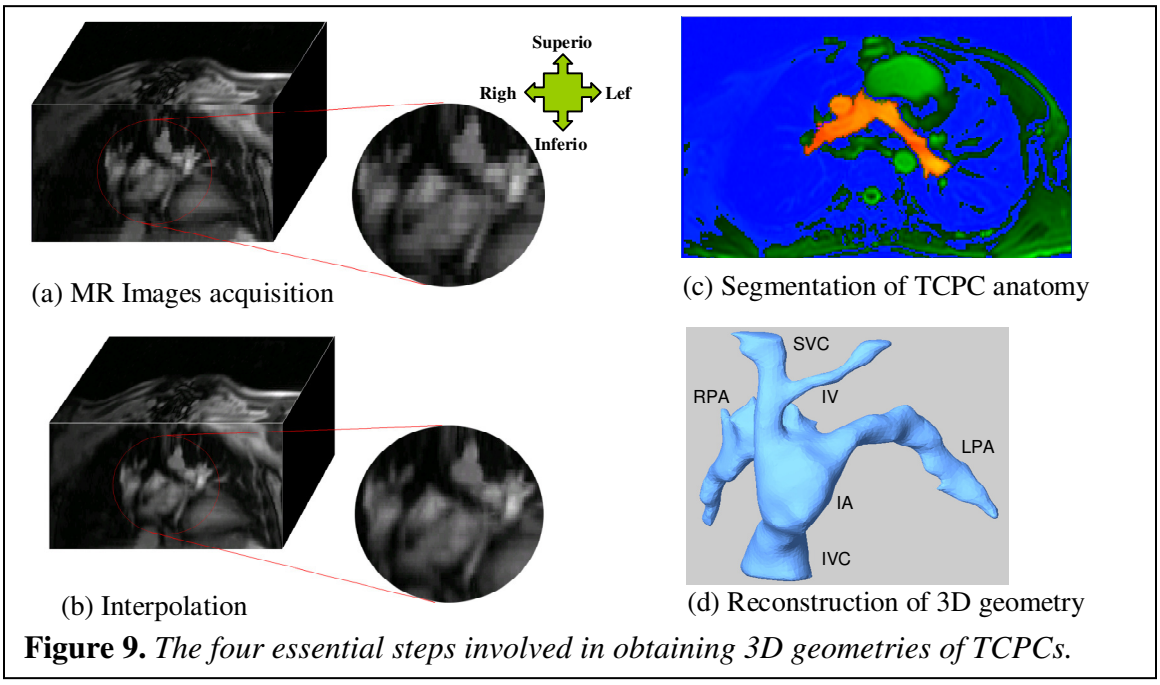

(a) MR Images acquisition

(c) Segmentation of TCPC anatomy

(b) Interpolation

(d) Reconstruction of 3D geometry

Figure 9. *The four essential steps involved in obtaining 3D geometries of TCPCs.*

B.1) Interpolation

In our application, the TCPC geometry is extracted from MR images. These typically have an out-of-plane resolution that is lower than the in-plane. In order to optimize the accuracy of the vessel segmentation, the raw MR images are first interpolated in the out-of-plane direction to compensate for the lower resolution. This is done using an interpolation method that was developed in our laboratory, the adaptive control grid interpolation (ACGI) technique[1] (Figure 3a), and that was shown to perform better than traditional interpolation strategies using either spline or linear interpolation schemes. I constantly edited the code to manipulate MRI data to acquire interpolated images from the raw dicom files obtained.

B.2) Segmentation

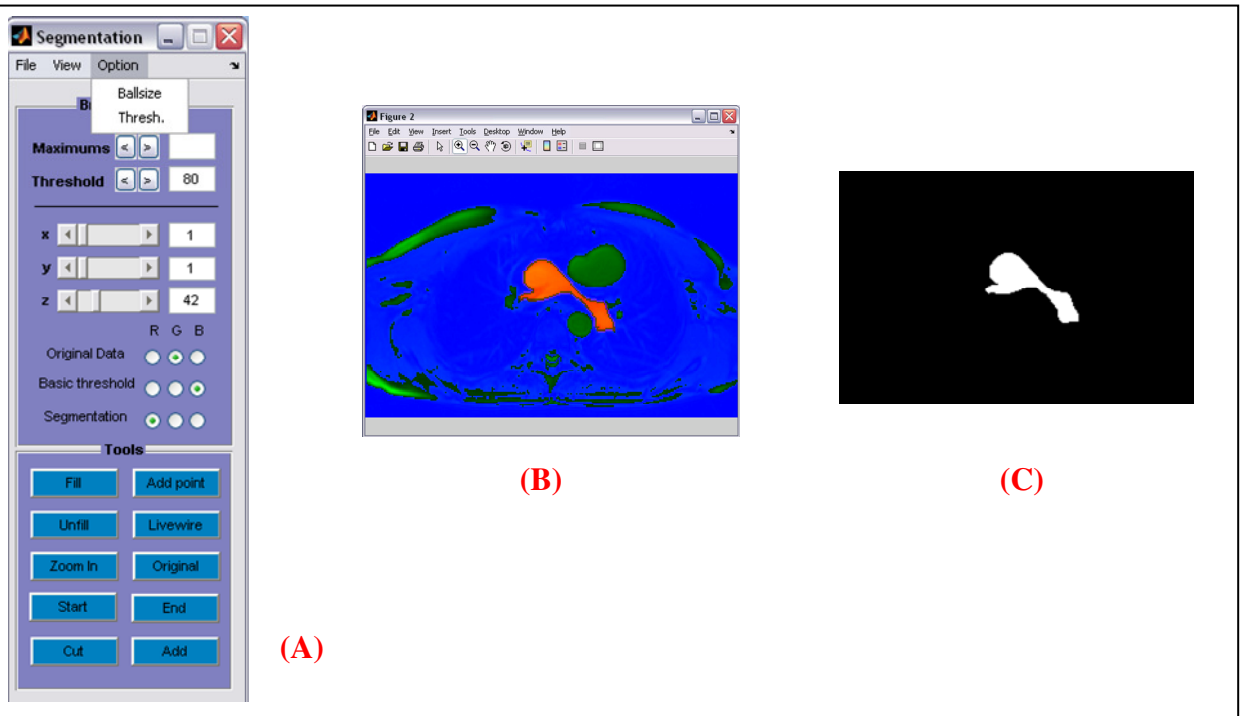

Figure 10. *The segmentation GUI (A), segmented slice of MRI with RGB contrast settings (B), and segmented slice with black and white contrast before saving as bmp (C).*

After interpolation, the vessels of interest (venae cavae and pulmonary arteries) are segmented out of the enhanced MRI dataset. This is done using a shape-element segmentation technique, called bouncing-ball. In this approach, the MR image may be considered as a 3D map, where the slope is dictated by the intensity gradients of the MRI rather than by the changes in elevation. Sharp changes in intensity (when going from a vessel lumen to the surrounding tissues for example) appear as steep slopes, whereas regions of uniform intensities appear as valleys. A segmentation element in the shape of a ball is released in the lumen of the vessel of interest, with an initial random velocity (Figure 10B). It bounces against the steep slopes until the whole vessel lumen is segmented. A larger ball will segment the vessel faster as well as ensure that the segmentation does not leak into nearby vessels, while a smaller ball could segment much smaller vessels, but has the risk of capturing surrounding regions.

This in-house bouncing ball algorithm has been modified to not only segment one MR image slice at a time but many slices at a time. The ball now bounces off the walls of the vessel and moves along the z-plane at the same time segmenting a larger part of the vessel. By clicking ‘Start’ and segmenting the first MRI slice, segmenting the last slice, and then clicking ‘End,’ the user will be able to segment all the slices in between them as well by linear interpolation saving time and speeding up the segmentation process.

The livewire is an option also provided in the segmentation tool. It uses Dijkstra's algorithm to connect two pixels in the image by the shortest possible path. In the process, it creates a boundary (steep slope) for the bouncing ball, removing unwanted vessels in the segmentation. Recently, modification has been made to decrease the value of the ‘livewired’ pixels to decrease their values by 20 instead of removing the pixels straight away. Previously, once the pixels were set to zero, the next livewire in that area became difficult. Now, livewire

has been modified to become more flexible with surrounding conditions. In addition to those tools, we developed 'Cut' and 'Add' functions to the Graphic User Interface (GUI), as shown in Figure 8, to cut and add a pixel at a time respectively. This was implemented since the livewire tool was not stable and livewire was not functional at the boundaries of the MRI scans. We also needed to add pixels in the segmentation process to add details to certain poor MRI scans as well as undo mistakes when using either livewire or Cut tools. When adding a pixel, the point will increase in value by 20 each time you click on it and when removing a pixel, the point will decrease in value by 20.

B.3) 3D TCPC Database

In our laboratory, a database of over 250 patients has been created as part of an ongoing study seeking to better understand the Fontan hemodynamics and improve the TCPC design. This database contains anatomical PC MRI and necessary clinical information from 3 major hospitals in the United States - Egleston Hospital, Atlanta (CHOA), Children's Hospital of Philadelphia (CHOP) and University of North Carolina (UNC).

In this study, 26 patients, 13 each of intra-atrial and extra-cardiac, were chosen. Details of these patients are shown in the following tables.

Table 1. *Intra-cardiac patients' diagnosis*[26].

Patient	Diagnosis	Fontan Type	Hemi/BDG	BSA (m^2)	Age (yrs)
CHOA 004	HRHS, TA, VSD, PS	IA	BDG	0.56	3

CHOA 009	SV-DI AV connection	IA, DSK	BDG	0.58	2
CHOA 011	HLHS	IA - Fenestrated	BDG	1.21	11
CHOA 027	HRHS, TGA, TA, VSD, LPA hypoplasia	IA, DSK, Fenestrated	BDG	0.56	2
CHOP 008	HLHS	IA	Hemi	1.94	16
CHOP 018	HLHS, ASD	IA	Hemi	1.23	12
CHOP 030	TA, VSD	IA	Hemi	1.32	10
CHOP 034	HRHS, SV, DX, TA, VSD, PS	IA	Hemi	1.19	11
CHOP 037	PA, HRHS	IA	Hemi	1.49	15
CHOP 068	HLHS	IA	Hemi	0.94	6
CHOP 073	HLHS	IA	Hemi	0.963	9
CHOP 092	HLHS, TGA, Hypoplastic AA, VSD	IA - Fenestrated	Hemi	0.495	1

CHOP 096	PA	IA - Fenestrated	BDG	1.063	10

IA -intra atrial; Hemi - hemi-Fontan; BDG - bidirectional glenn; HRHS - hypoplastic right heart syndrome; HLHS - hypoplastic left heart syndrome; TA - tricuspid atresia; ASD - atrial septal defect; VSD - ventricular septal defect; SV - single ventricleAV - atrioventricular; DI - double inlet; TGA - transposition of great arteries; DX – dextrocardia; AA - aortic arch; PA - pulmonary atresia; PS - pulmonary stenosis; DSK - Damus-Stansel-Kaye procedure

Table 2. *Extra-cardiac patients' diagnosis*[26].

Patient	Diagnosis	Fontan Type	Hemi/BDG	BSA (m^2)	Age (yrs)
CHOA 007	HLHS	EC	BDG	0.79	6
CHOA 008	HRHS, TA	EC	BDG	0.69	5
CHOP 006	HLHS	EC	Hemi	1.05	10

CHOP 007	HRHS, Ebstein's anomaly	EC, DSK-ASD repair	BDG	1.02	8
CHOP 013	HLHS, ASD	EC	Hemi	0.83	6
CHOP 067	SV - DI LV, VPS - TGA	EC	BDG	1.064	9
CHOP 085	HLHS	EC	BDG	0.589	3
CHOP 088	DX, Juxtaposition of atria appendages, TA, TGA, AA hypoplasia	EC - Fenestrated	BDG	0.544	3
CHOP 089	TA, VSD	EC - Fenestrated	BDG	0.872	7

CHOP 090	PA, IVS, RV - Hypertrophy	EC - Fenestrated	BDG	1.152	8
CHOP 091	DO – RV, IVS, MA, PA	EC - Fenestrated	BDG	0.994	8
CHOP 095	DI LV, PA	EC - Fenestrated	BDG	1.253	8
CHOP 116	Ebstein's anomaly	EC	BDG	0.793	8

EC – extra cardiac; Hemi - hemi-Fontan; BDG - bidirectional glenn; HRHS – hypoplastic right heart syndrome; HLHS - hypoplastic left heart syndrome; TA - tricuspid atresia; ASD - atrial septal defect; VSD - ventricular septal defect; SV - single ventricle; LV – left ventricle; RV - right ventricle; DI - double inlet; DO - Double Outlet; TGA – transposition of great arteries; DX – dextrocardia; AA - aortic arch; PA - pulmonary atresia; DSK - Damus-Stansel-Kaye procedure; MA -Mitral Atresia; IVS - intact ventricular septum

B.4) Generation of 3D TCPC Geometries with Centerlines

The following are the 3D TCPC geometries generated together with the centerline along the SVC, IVC, LPA and RPA.

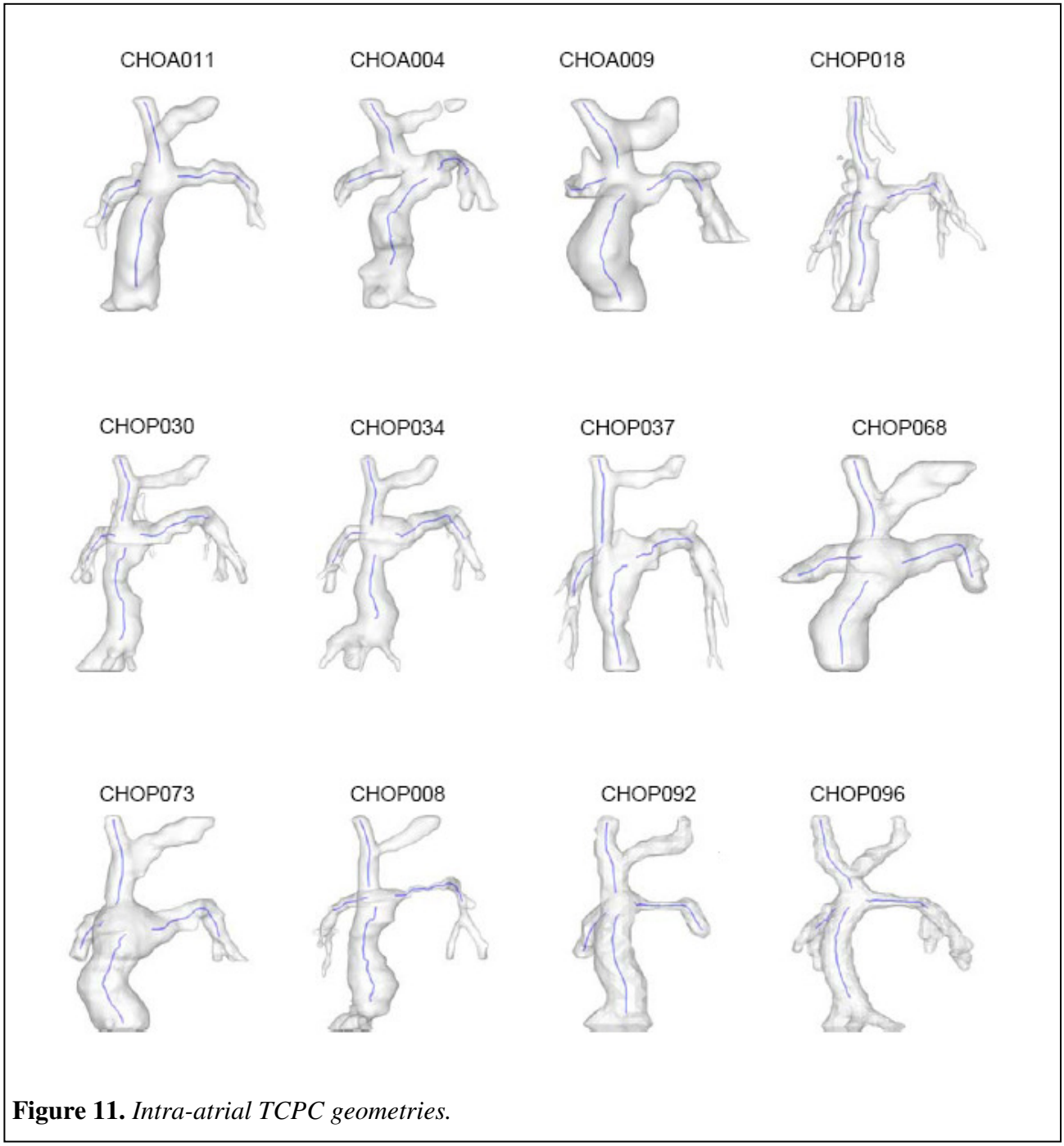

Figure 11. *Intra-atrial TCPC geometries.*

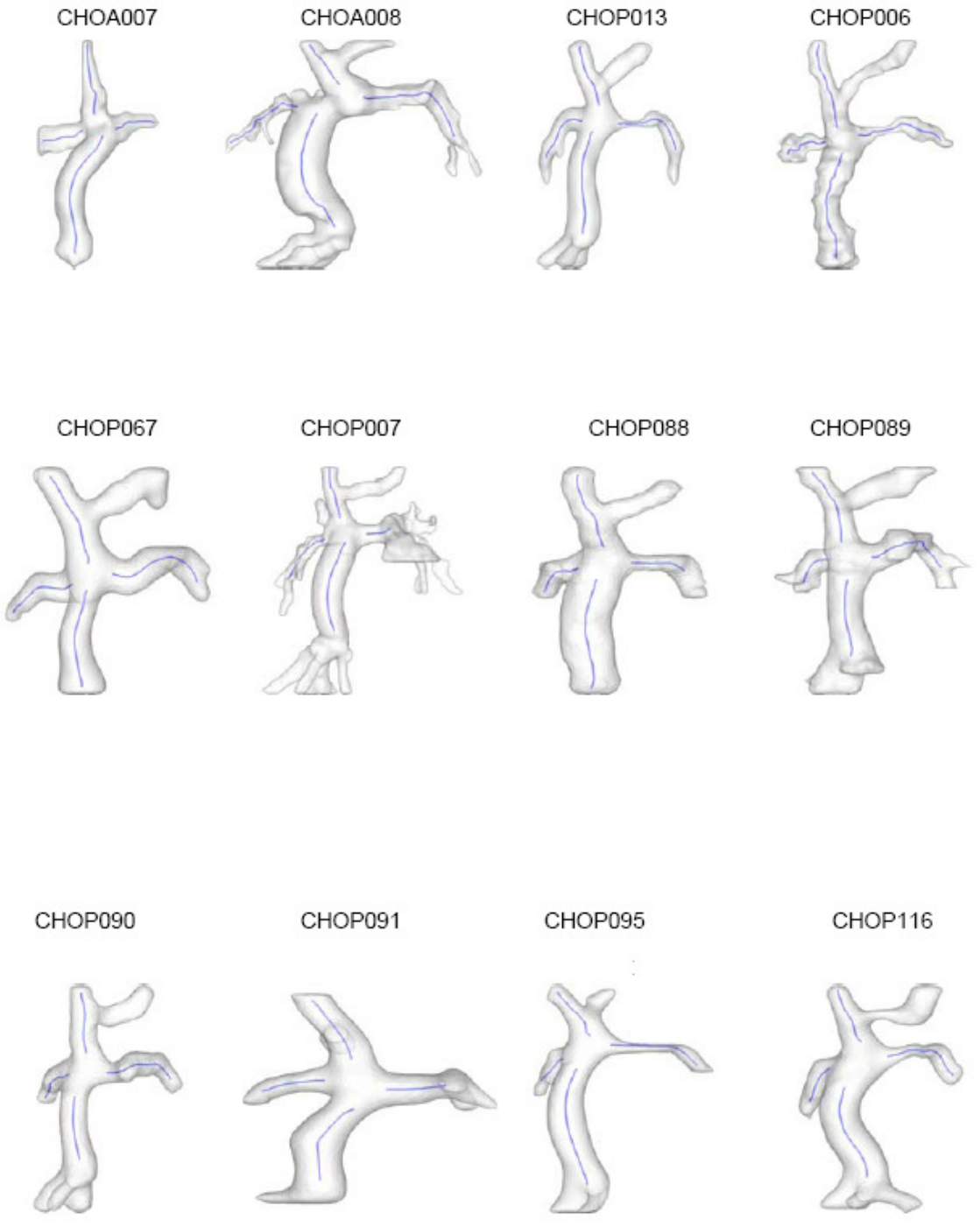

Figure 12. ***Extra-cardiac TCPC geometries.***

B.5) Discussion

Extra-cardiac and intra-atrial anatomies result from different approaches to the surgical reconstruction of the Fontan baffle as described earlier. However, results show that there is no significant difference in their baffle sizes. Instead the difference appears to be a higher standard deviation of the baffle cross-sectional area along its length in intra-atrial TCPCs when compared to extra-cardiac TCPCs. In conclusion, the intra-atrial baffle always has larger cross-sectional fluctuations than the extra-cardiac conduit, which is to be expected as the former is constructed using part of the right atrium while a smooth and uniform graft conduit is used for the latter. The large standard deviation of the IVC cross-sectional areas observed in the intra-atrial TCPCs could also be the reason why there was no statistical significance between the IVC dimensions in intra-atrials and extra-cardiacs. No trends in the standard deviations of LPA and RPA could be detected.

Intra-atrial patients showed significantly higher values in the ratio of mean cross-sectional areas of RPA to SVC, which is possibly because the TCPC junction for the intra-atrial and extra-cardiac are not located at the same point on the native RPA. The native RPA anatomically decreases in diameter toward the right side, and the location on the RPA where the TCPC is constructed for the intra-atrial is possibly slightly shifted toward the left side compared to the extra-cardiac TCPC. From a hemodynamic standpoint, the closer the TCPC is to the main pulmonary artery (MPA), the larger the PA sizes will be and thus the lesser the overall constriction in the flow transport.

There was no statistical significance in the curvature of the vessels at the meeting point of the TCPC junction. The discrepancy in data was due to some TCPCs in which the RPA was

more curved than the other anatomies. This shows that the Fontan procedure depended heavily on the patient's anatomy and body-type as much as on the best connection seen by the surgeon.

As depicted, the intra-atrial Fontans have lower collinearity (nearly significant) value than their EC counter parts. Collinearity values approaching zero can be interpreted as their IVC and SVC are oriented in a head on collinear manner. So intra-atrial Fontans have an increased chance of flow stagnation and highly unsteady and dissipative interaction between the colliding flows, compared to that in extra-cardiacs where the power losses seem to occur along the walls.

C) *Specific Aim 1:* Surgical Planning of Complex Congenital Heart Defects Using MRI and 3D Segmentation

In vitro, in vivo and animal studies have demonstrated the Greta sensitivity of the TCPC efficiency to its design, suggesting possible improvements such as including a caval offset, flaring the connection sites, etc. Taking this one step further, the cardiovascular fluid mechanics laboratory has undertaken the task of developing a surgical planning tool that would allow the surgeon to optimize the connection for every single patient. The major components of this tool development are to first reconstruct the patient's cardiovascular anatomy, then to be able to edit and modify the vessels so as to perform virtual surgeries, and to finally assess the efficiency of the different options retained.

C.1) Surgical Planning

The reconstructed anatomy is meant to be used for surgical planning. With the assistance of Dr. Rossignac, in Georgia Tech's College of Computing, and his team, a tool (SURGEM®[6]) has been developed to manipulate the 3D model of the patient's reconstructed cardiovascular

system and to try out different surgical configurations[3]. I provided complete 3D segmentations of the heart and surrounding vessels as one data set so that they can be superimposed with the 3D geometry of the TCPC to evaluate and configure the Fontan connection. Two magnetic trackers allow for the 3D anatomical orientation and interactive deformation of the anatomy and of the graft used to perform the final stage of the TCPC. An example of such procedure is given in Figures 13 and 14. Using two magnetic trackers, the surgeon can grab the vessels and deform them to the desired shape (Figure 13), or try out different potential locations for the IVC graft (Figure 14)[5]. The tool exhibits high efficiency and robustness. Once the surgeon has the desired configuration, the new vascular configuration can then be tested with the Image-based surgical planning system to see how well the new surgical procedure would perform[4].

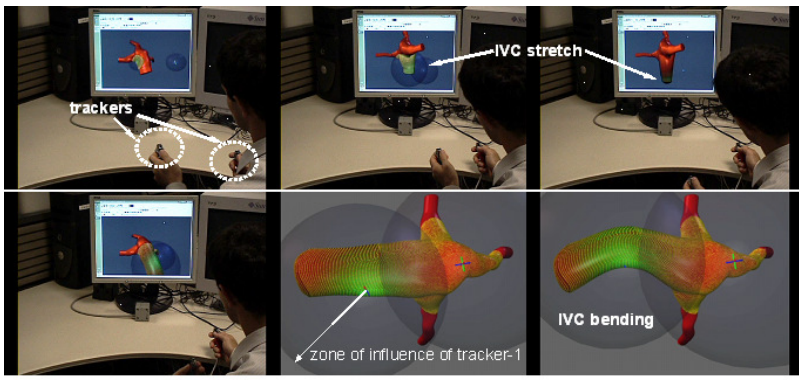

Figure 13. *The preliminary operation of the surgical interactive surface modification tool, SURGEM®, for surgical planning of patients in the Glenn stage*[1].

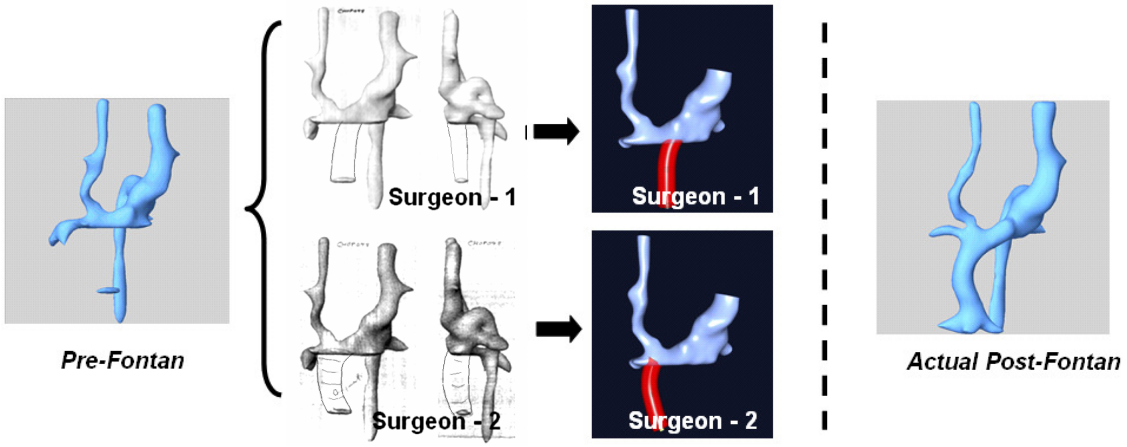

Figure 14. *Sketches aiding in pre-surgery planning*[1].

C.2) Complete Anatomical Reconstruction

So far, surgical planning operations and modeling were done using only the cardiovascular structures of direct interest, namely the pulmonary arteries and venae cavae. However, SURGEM® would offer a more realistic representation of the surgical constraints that the surgeon will encounter during the operation if it included more information such as the position of the heart, aorta and pulmonary veins.

Given the time needed to segment that many additional structures, the option retained to address that issue was to reconstruct only the vessels of direct interest, but also provide the surgeons with a picture showing the 3D reconstructions superimposed on MR image slices (Figure 15). Additionally, a movie was captured of the MR image and 3D reconstruction superimposed rotating such that surgeons could observe both anterior and posterior ends of the patient.

Figure 15. *Left: interpolation based on axial, Middle: interpolation based on axial, coronal, and sagittal, Right: Glenn reconstructions with MR Images superimposed.*

As part of the preliminary work for this project, an attempt was made to segment out all the structures of interest and provide the whole cardiovascular structure to the surgeons. The following steps were employed in segmenting the structures of interest.

Step 1: Segment the superior and inferior vena cavae with the left and right pulmonary arteries (TCPC)

Step 2: Export the segmentation files (in bitmap format) to Materialise Mimics 9.1 to make the 3D reconstructions, using specific interpolated slice distance and pixel size which depend on the MRI scan

Step 3: Edit the 3D segmentation using editing tools in Mimics to make the reconstruction smoother and more distinct

Step 4: Save the 3D geometries in STL format

Step 5: Repeat steps 1-4 segmenting just the surrounding parts which include the heart, aorta and pulmonary veins

Step 6: Export both STL files to Geomagics superimposing both geometries

Step 7: Save the superimposed geometries as one STL image

Step 8: Repeat steps 1-7 for the same patient in the Glenn stage (pre-Fontan)

The above procedure was applied on two commonly encountered trends in Fontan patients- severe LPA stenosis due to aortic arch reconstruction and large IVC-to-LSVC offset in dual SVC cases (Figures 16 and 17).

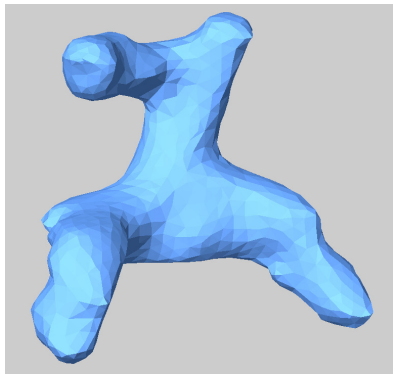

(a) Glenn

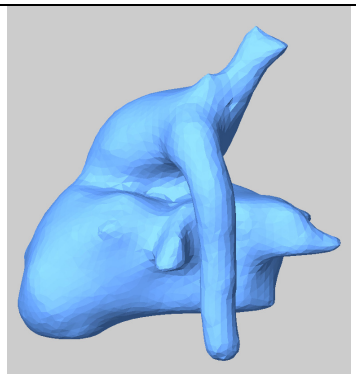

(b) Heart with aorta and pulmonary veins

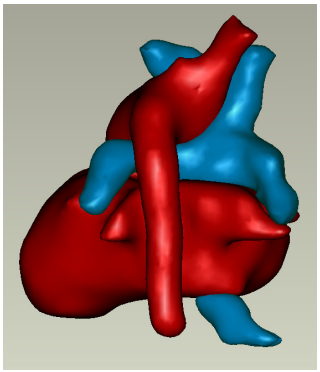

(c) Complete 3D geometry

Figure 16. *STL file of Children's Hospital of Philadelphia (CHOP) 57 3D geometry of (a) Glenn superimposed with (b) heart, aorta and pulmonary veins to give (c) the complete anatomical reconstruction required.*

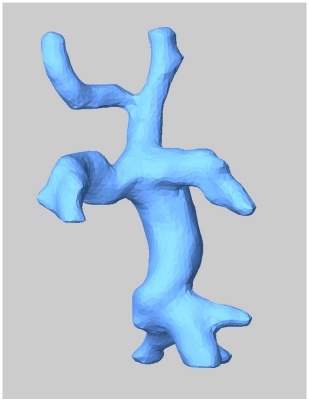

(a) Glenn

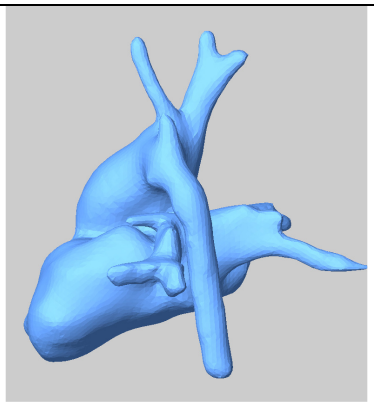

(b) Heart with aorta and pulmonary veins

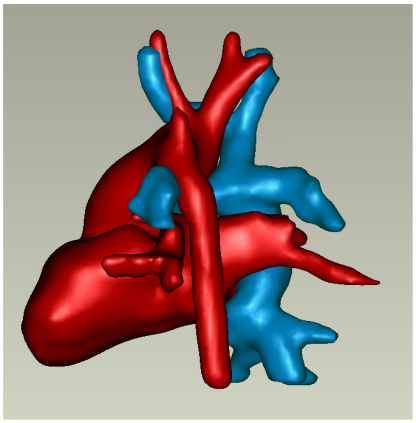

(c) Complete 3D geometry

Figure 17. *STL file of CHOP 84 3D geometry of (a) TCPC (superimposed with (b) heart, aorta and pulmonary veins to give (c) the complete anatomical reconstruction required.*

C.3) Limitations

In his virtual design, the surgeon chose to include an offset, which had previously been shown to be beneficial in terms of power losses[26]. This however is not the case here and the

energy losses computed in the virtual extra-cardiac anatomy (1.36mW) were actually higher than those computed for the actual post-operative anatomy (0.58mW). The primary reason for this increased energy dissipation is the smaller sized baffle used in the virtual design when compared to the actual one. Energy losses in the virtual design could have been lowered further by increasing the baffle size. However, it has also been shown that important mismatches between the baffle size and the diameters of the connecting vessels yielded detrimental flow features such as regions of flow stagnation or recirculation[25].

For a proper surgical-planning scenario, the surgeon should thus have tested-out several baffle sizes and used the results of the corresponding CFD simulations to decide which one was optimal, as there is a tradeoff between reduced power losses and increased adverse flow features. In addition it has been previously shown that small differences under resting conditions may actually have a large impact in exercise situation when increased cardiac output would result in increased energy losses.

There are also limitations to the segmentation technique used to extract relevant structures of Fontan patients. Since the segmentation tool is only able to extract the 3D geometry of blood flow within the vessels, it does not reconstruct the actual 3D geometry of the heart which includes the thick muscular walls. Furthermore, the livewire function in the segmentation tool used to remove unnecessary parts of the MR image cannot be used at the edges of the segmentation window. Improvements to the algorithm and code could improve the accuracy of the complete anatomical reconstructions. This would eliminate unnecessary steps to smooth the reconstruction in Mimics.

Additionally, to maintain the continuity and smoothness of reconstructions, 2 slices before and after the slice being segmented are also segmented (indicated by contrasting orange).

Due to this feature, details are lost in the 3D reconstructions. This problem is most common when segmenting the aorta. The pulmonary veins and the aorta get stuck together. Mimics is needed to edit and ensure the aorta is prominent and separated. An option of segmenting the slices one at a time could be added into the Graphical User Interface (GUI) (see Figures 16 and 17) to solve the problem of densely packed structures appearing as one structure in the reconstruction.

C.4) Future Work

Thus, minimum LPA diameter is the most distinguishing geometric parameter between intra-atrial and extra-cardiac TCPCs. Based on this study, we could combine this application of geometrical studies with the *in vivo* hemodynamics study done in the lab to understand how these significantly impact the patient's cardiac output due to power loss. Preliminary results obtained from such experiments are shown in Figure 18, where for the first time, power losses have been evaluated in the TCPC *in vivo* using PC MRI. Lack of compliance and contractility within the extra-cardiac could partly contribute towards these differences in the power losses compared to the more dynamic intra-atrial TCPCs. It should be noted that the power losses evaluated in this plane are 2D without taking into account the derivatives in the through-plane direction. This is because the slice thickness is 5 mm, which is too large for computing the derivatives accurately.

To get around this issue, a divergence free interpolation scheme is used. By registering the anatomic reconstruction with the vector field obtained using these coronal slices, it will be possible to reconstruct the 3D time varying flow fields in the TCPC. However, the lab faces challenges such as the time taken to calculate the vector flow fields. It takes a long time to

combine the hemodynamics results with the surgical planning proposed in Specific Aim 1 so that the surgeon can make an informed decision before operating on the patient.

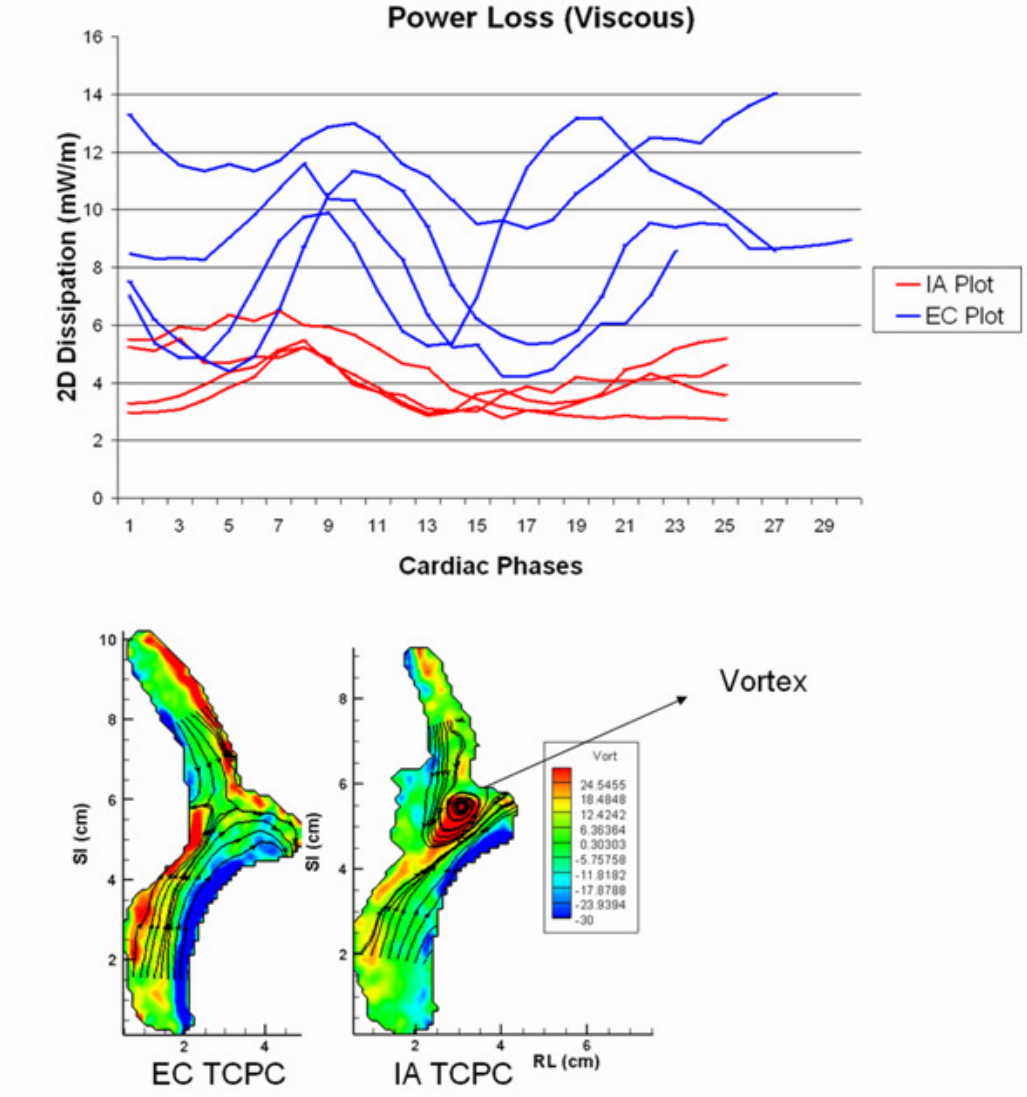

Figure 18. *Dissipation plot (top) and vorticity plots for an extra-cardiac and intra-atrial TCPC. Vortices present in the pouch region of the intra-atrial TCPC were responsible for energy losses while for the extra-cardiacs losses took place along the walls*[25].

Different views of the 3D TCPC and full segmentation geometries would help surgeons understand the anatomy much better than before. This is achieved through "Display Pipeline," a technique that refers to transformation of the object data from its original defined space through a series of mappings until its final expression on the screen coordinate system. Computing of

illumination, clipping of data to view volume and perspective transformation are some of the tools employed.

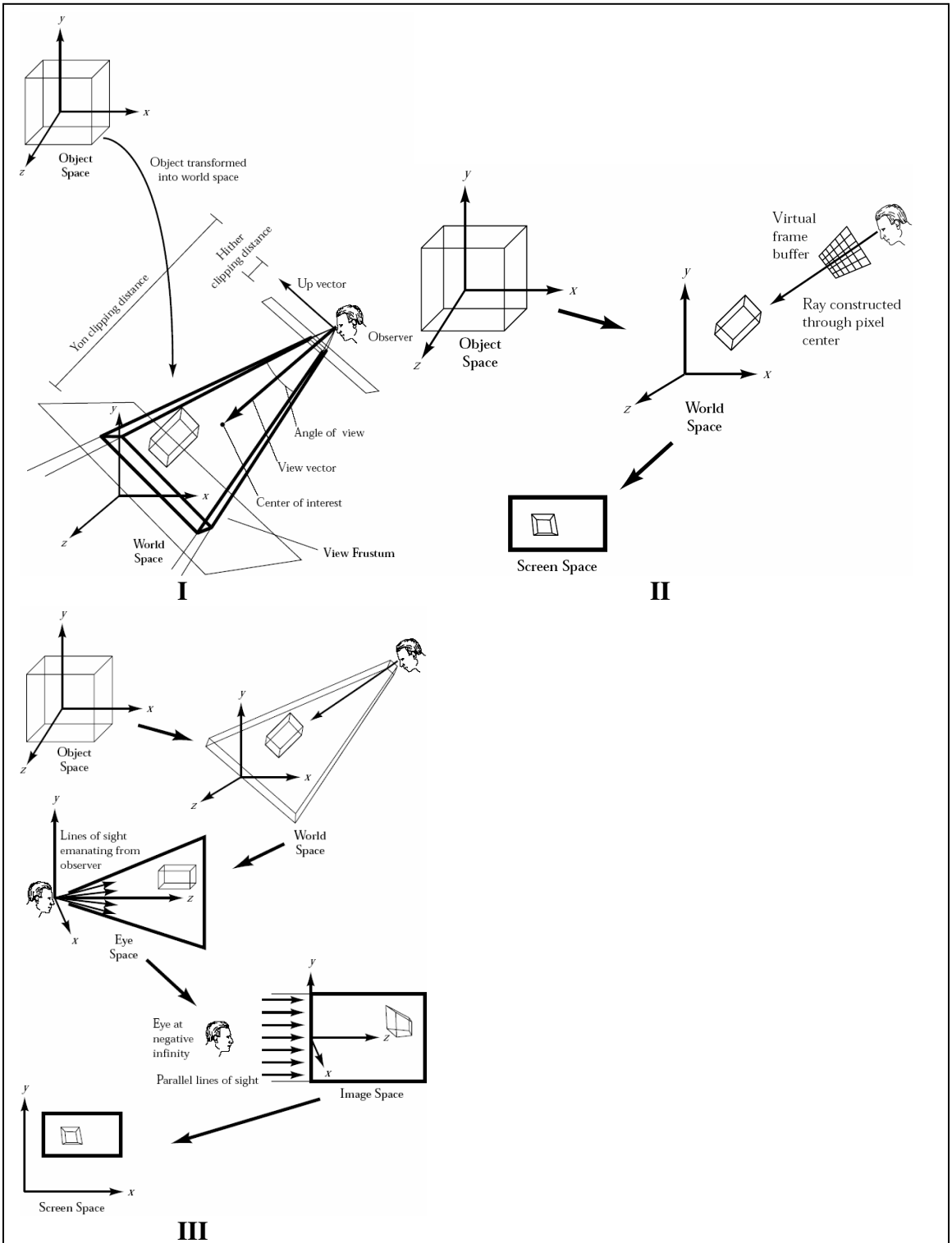

Figure 19. *Object to world space to view frustum (I), ray casting (II), and change of perspective (III)*[27].

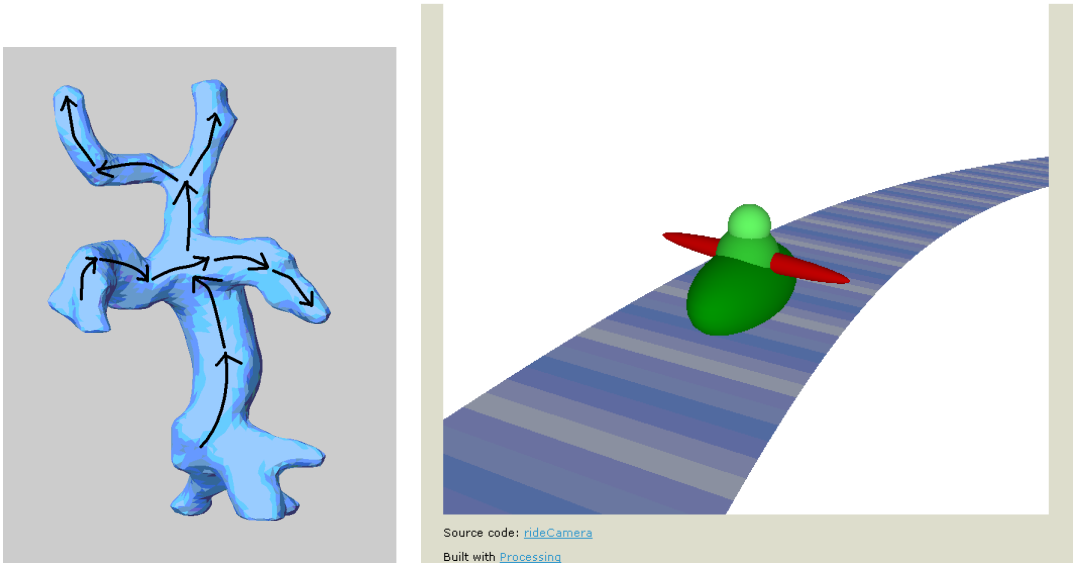

Figure 20. *How the 3D ride program implemented with the points of the TCPC as a possible pathway.*

This would enable surgeons to change views and also be able to view the interior of the segmented 3D geometry. "3D ride," a program implemented with Processing[27] (Figure 20) enables one to decide the path in 3D by selecting the points of the geometry and then go along the path. By selecting the points within the lumen of the LPA, RPA, SVC and IVC, one could view the segmentation from within. This will be an artificial simulation of the red blood cell (RBC) going through the vessels. The perspective can also be changed by the movement of the mouse (moving upwards would zoom in and moving downwards would zoom out).

D) Conclusion

The main goal is to create a more realistic and practical pre-surgical planning tool which is faster and more accurate. The tool will help surgeons get more familiar with the patient's anatomy before surgery. This study is also targeted in the study of differences in power losses that occur in intra-atrial and extra-cardiac TCPCs. Different scenarios can be discussed with peers giving more time than in the emergency room. A database of possible surgeries and solutions envisioned by different surgeons could be created which surgeons could use as models and references in the future. This should speed up the improvements in pre-surgical planning and the design of the TCPC in Fontan surgeries.

E) Acknowledgements

- National Heart and Lung Blood Institute Grant HL67622
- M. D., S. Sharma, M. D. and M.A. Fogel, M. D. , Cardiologists
- Ajit P. Yoganathan, Ph. D , Faculty Advisor
- Kartik Sundareswaran, Mentor
- Diane de Zelicourt, Mentor
- Jeffrey O. Donnell, LCC 4700 Instructor
- Douglas B. Williams, Faculty Mentor

F) References

1. Yoganathan A., "National Heart and Lung Blood Institute Grant HL67622," 100-156, Aug, 2006.
2. Fontan, F., and E. Baudet, Surgical repair of tricuspid atresia: Thorax, 1971; 26: 240-248.
3. Rossignac J. and Novak, M., Research issues in model-based visualization of complex data-sets. IEEE Computer Graphics & Applications, 1994. 14(2): p. 83-85.
4. Rossignac J., Representing and visualizing complex continuous geometric models, in Scientific Visualization: Advances and Challenges Eds. L. Rosenblum, 1994, Academic Press, p. 337-348.
5. Rossignac J. and O'Connor, M., SGC: A dimension-independent model for pointsets with internal structures and incomplete boundaries, in Geometric Modeling for Product Engineering,Eds. North-Holland, 1989, p. 145-180.
6. Rossignac J., Through the cracks of the solid modeling milestone, in From Object Modeling to Advanced Visualization,Eds. S. Coquillart, W. Strasser and P. Stucki, 1994, Springer Verlag, p. 1-75.
7. S. LeRoy RN, MSN, L. Callow RN, MSN, CPNP, K. George RN, MSN, CPNP, E.Bove, MD, D. Crowley, MD. C.S. Mott Children's Hospital: Congenital Heart Center: Hypoplastic Left Heart Syndrome. http://www.med.umich.edu/mott/chc/patient_con_hyp.html (July 2000).
8. S. LeRoy RN, D. Crowley, MD. C.S. Mott Children's Hospital: Congenital Heart Center: Tricuspid Atresia. http://www.med.umich.edu/mott/chc/patient_con_hyp.html (April 2003).
9. Fatouraee N, Amini AA. Regularization of flow streamlines in multislice phase-contrast MR imaging. IEEE Trans Med Imaging 2003; 22(6):699-709.
10. Dodu F, Rabut, C. Irrotational or Divergence Free Interpolation. Numerical Mathematics 2004; 98:477-498.

11. Song SM, Leahy, R.M Computation of 3-D velocity fields from 3-D cine CT images of the human heart. IEEE Trans Med Imaging 1991; 10(4):295-306.
12. Khairy P, Poirier N, Mercier LA. Univentricular heart. Circulation. 2007;115(6):800-812.
13. Haas, G. S., H. Hess, M. Black, J. Onnasch, F. W. Mohr, and J. A. van Son, Extracardiac conduit fontan procedure: early and intermediate results: Eur J Cardiothorac Surg, 2000; 17 (6): 648-54.
14. Petrossian, E., V. M. Reddy, D. B. McElhinney, G. P. Akkersdijk, P. Moore, A. J. Parry, L. D. Thompson, and F. L. Hanley, Early results of the extracardiac conduit Fontan operation: J Thorac Cardiovasc Surg, 1999; 117 (4): 688-96.
15. Tam, V. K., B. E. Miller, and K. Murphy, Modified Fontan without use of cardiopulmonary bypass: Ann Thorac Surg, 1999; 68 (5): 1698-703; discussion 1703-4.
16. Shiota, T., R. Lewandowski, J. E. Piel, L. S. Smith, C. Lancee, K. Djoa, N. Bom, A. Cobanoglu, M. J. Rice, and D. J. Sahn, Micromultiplane transesophageal echocardiographic probe for intraoperative study of congenital heart disease repair in neonates, infants, children, and adults: Am J Cardiol, 1999; 83 (2): 292-5, A7.
17. Fogel, M. A., P. M. Weinberg, A. J. Chin, K. E. Fellows, and E. A. Hoffman, Late ventricular geometry and performance changes of functional single ventricle throughout staged Fontan reconstruction assessed by magnetic resonance imaging: J Am Coll Cardiol, 1996; 28 (1): 212-21.
18. Fogel, M. A., P. M. Weinberg, J. Rychik, A. Hubbard, M. Jacobs, T. L. Spray, and J. Haselgrove, Caval contribution to flow in the branch pulmonary arteries of Fontan patients with a novel application of magnetic resonance presaturation pulse: Circulation, 1999; 99 (9): 1215-21.
19. Salim, M. A., T. G. DiSessa, K. L. Arheart, and B. S. Alpert, Contribution of superior vena caval flow to total cardiac output in children. A Doppler echocardiographic study: Circulation, 1995; 92 (7): 1860-5.
20. Be'eri E, Maier SE, Landzberg MJ, Chung T, Geva T. In vivo evaluation of Fontan pathway flow dynamics by multidimensional phase-velocity magnetic resonance imaging. Circulation. 1998;98(25):2873-82.
21. Sharma, S., A. E. Ensley, K. Hopkins, G. P. Chatzimavroudis, T. M. Healy, V. K. Tam, K. R. Kanter, and A. P. Yoganathan, In vivo flow dynamics of the total cavopulmonary connection from three-dimensional multislice magnetic resonance imaging: Ann Thorac Surg, 2001; 71 (3): 889-98.
22. Frakes, D. H., Pekkan, K., Smith, M.J.T., Yoganathan, A. Three-Dimensional Velocity Field Reconstruction. J. of Biomechanical Eng. 2004; 126:727-735.
23. Healy, T. M., C. Lucas, and A. P. Yoganathan, Noninvasive fluid dynamic power loss assessments for total cavopulmonary connections using the viscous dissipation function: a feasibility study: J Biomech Eng, 2001; 123 (4): 317-24.
24. Paik DS, Beaulieu CF, Jeffrey RB, Rubin GD, Napel S. Automated flight path planning for virtual endoscopy. Med Phys. 1998;25(5):629-37.
25. Sundareswaran, K.S.; de Zelicourt, D.; Pekkan, K.; Jayaprakash, G.; Kim, D.; Whited, B.; Rossignac, J.; Fogel, M.A.; Kanter, K.R.; Yoganathan, A.P. Anatomically Realistic Patient-Specific Surgical Planning of Complex Congenital Heart Defects Using MRI and CFD. 2007; 202 – 205.

26. Krishnankutty, R.R. Quantification and Analysis of the Geometric Parameters of the Total Cavo Pulmonary Connection Using a Skeletonization Approach. 2007; 118-143.
27. Rossignac J., 3D Mesh Compression, Visualization Handbook, 2005.